Theoretical Computer Science 457 (2012) 76–85

Contents lists available at SciVerse ScienceDirect

Theoretical Computer Science

journal homepage: www.elsevier.com/locate/tcs

Two-robot source seeking with point measurements☆

Yotam Elor*, Alfred M. Bruckstein

Faculty of Computer Science and the Goldstein UAV and Satellite Center, Technion, Haifa 32000, Israel

ARTICLE INFO

Article history:
Received 12 November 2011
Received in revised form 4 June 2012
Accepted 20 June 2012
Communicated by D. Peleg

Keywords:
Source-seeking
Point measurement
Gradient
Fume tracking

ABSTRACT

A source-seeking process for a pair of simple, low capability robots using only point measurements is proposed and analyzed. The robots are assumed to be memoryless, to lack the capability of performing complex computations and to have no direct communication abilities. Their only implicit form of communication is by sensing their relative position and the only response of a robot to the point measurement it makes is by moving to adjust its distance to the other robot according to a predetermined rule. The proposed algorithm is robust: we prove that the algorithm performs correctly even when the robots frequently err due to noisy sensor readings.

© 2012 Elsevier B.V. All rights reserved.

1. Introduction

In this work we consider the problem of controlling a group of robots in order to find the maximum of a scalar function defined over the plane $z : \mathbb{R}^2 \to \mathbb{R}$. This problem is often called *source-seeking* with applications varying from finding the source of leakage of a hazardous chemical to modeling chemotaxis for primitive creatures. Roughly speaking, it is assumed that the value of the scalar function becomes weaker as one move away from the source.

Small (possibly nano) robots with very low capabilities are considered. Such small robots, even when equipped with multiple sensors, are unable to directly sense the gradient of $z(\cdot)$ because the spatial separation between its sensors is not large enough. Thus, it is assumed that the robots can only take point measurements of $z(\cdot)$. We limit the discussion to *memoryless*, or *reactive*, algorithms in the sense that an action performed by a robot is determined solely by the robot group's configuration at the time the action is taken. The robots cannot estimate the gradient by comparing the currently measured value to old values and cannot communicate directly, thus cannot explicitly share their point measurements. However, the robots are able to sense their relative positions.

Under the limitations above, it is obvious that a single robot cannot accomplish the task. We consider the smallest group which can perform the task, i.e. a group of two robots. When executing the proposed algorithm, every robot changes its position in order to maintain a certain distance from the other robot. The distance a robot desires to maintain is proportional to his currently measured value of $z(\cdot)$. Thus, the robot which senses a higher value will try to maintain a larger distance compared to the robot that senses a lower value. We shall show that this process will cause the pair of robots to drift toward higher values of $z(\cdot)$.

The main advantage of the *reactive* nature of the proposed algorithm is its robustness. We prove that the algorithm works even when the robots frequently make wrong moves due to noisy sensor readings. To the best of our knowledge, the algorithm proposed in [1] is the only alternative *reactive* gradient-following algorithm that was proposed in conjunction with a multi-robot system performing point measurements. However, in [1] every robot is assumed to have access to the values measured by all other robots.

☆ This research was supported by the Technion Goldstein UAV and Satellite Center and by the European Community's FP7-FET program, SMALL project.
* Corresponding author. Tel.: +972 52 3289659.
E-mail address: yotam.elor@gmail.com (Y. Elor).

0304-3975/$ – see front matter © 2012 Elsevier B.V. All rights reserved.
doi:10.1016/j.tcs.2012.06.036

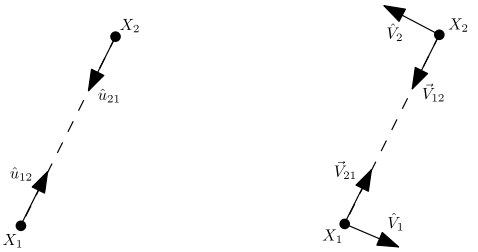

(a) Illustration of the notations. (b) Illustration of the induced velocities.

Fig. 1. Illustrations of the notations and induced velocities.

2. Related work

The *source-seeking* problem was studied under several sets of assumptions. Only the variant of the task in which the environment does not change in time will be discussed here. For a broader coverage see the excellent survey by Kowaldo and Russel [2].

Considering a single robot, the common method used to overcome the point measurement limitation is taking spatially separated measurements by moving the robot between readings. By "remembering" and subsequently comparing the readings, the robot can estimate the gradient [3–5]. Using computer simulations, Holland and Melhuish [6] studied simple algorithms inspired by the movement pattern of the *Escherichia coli* bacterium. Their algorithms are based on the simple "two-instant mechanism", i.e. at every time step, the robot compares the current reading with the previous one. Russel [7] studied motion patterns such as zigzag or hexagonal on the plane using the two instant mechanism. Using comparisons of two or three point measurements, several 2D and 3D motion patterns were proposed to accomplish source-seeking tasks, see [8,9].

When the robot moves, the measured value changes. Assuming continuous measurement, the time differential of the readings ($\dot{z}(\cdot)$) could be obtained as assumed in [10–17]. In [10,11], a hybrid controller is developed for the source-seeking task under noisy input assumptions. Matveev et al. [12,13] proposed a single robot algorithm in which the forward speed of the robots is fixed and the angular speed is controlled by $\dot{z}(\cdot)$. In their algorithm, the robot travels in spirals toward the maximum. Using a different angular speed control mechanism, Krstic and coworkers [14,15] have shown that the robot orbits the maximum of $z(\cdot)$ after reaching it. They have also extended their work to the 3D case [16]. A similar behavior can be achieved by controlling only the forward speed [17].

Considering a multi-robot system, Biyik and Arcak [4] addressed the scenario in which only one robot, the "leader", is able to sense the gradient of $z(\cdot)$. In their framework, the leader follows the gradient while the rest of the robots maintain a formation relative to the leader. When every robot is able to measure the gradient of $z(\cdot)$, variants of the Artificial Potential Field framework can be employed [18]. Gazi and Passino [19] studied the behavior of a swarm of robots affected by attraction, repulsion and gradient climbing forces. Using their proposed rules of motion the swarm maintains cohesiveness and travels in the direction of the gradient. Ogren et al. [20,21] considered a similar virtual forces mechanism combined with a Kalman filter to reduce noise. Bachmayer and Leonard [22] achieved similar results assuming each robot can measure the gradient only in the direction of motion ($\dot{z}(\cdot)$). Ghods and Krstic [23] considered the one-dimensional version of the problem. They proved that under their algorithm, the agents' density is highest around the source, thus the agents will deploy around it.

Mesquita et al. [24] proposed to solve the problem of finding the global maximum of a scalar function using many robots performing a biased random walk. Their work is based on the observation that when the speed of movement of the robots is inversely proportional to the value of the scalar function, the robots tend to spend more time in high-value areas.

As mentioned in the introduction, an algorithm resembling ours can be found in [1]. There, N robots maintain a uniform circle formation. By comparing the values they measure, the robots in the formation move with the gradient. However, in contrast to our work, in [1] every robot is assumed to have access to the values measured by all other robots.

3. The proposed source-seeking algorithm

Some notations are presented before formally describing the algorithm. The system comprises two robots denoted by r_1,r_2. The location of robot r_i in a global coordinate frame is given by X_i. The distance between the robots is denoted by D and given by $D = \|X_2 - X_1\|$ where $\|\cdot\|$ is the Euclidean norm. Let $\hat{u}_{ij}$ be the following unit vector $\hat{u}_{ij} = \left(X_j - X_i\right)/D$. The center of mass point is given by $CM = \frac{1}{2}(X_1 + X_2)$. When we explicitly add t to the indices of a quantity we refer to the value of that quantity at time t, e.g. $X_i(t)$ is the location of robot r_i at time t. The notations are illustrated in Fig. 1a.

Let $z(X)$ be the value of the scalar function at point X. It is assumed that for any X, $0 < z(X) < \infty$. Let $z_i = z(X_i)$ and let $D_i = f(z_i)$ be the desired distance for robot r_i, i.e. while executing the algorithm, robot r_i attempts to keep a distance of D_i from robot r_j. f is a positive strictly increasing function with bounded derivative, $0 < \frac{df}{dz_i} \leq 1/\max\{\|\nabla z\|\}$. The function f is user designed and affects the system behavior. We shall show that the algorithm achieves source-seeking for any function having the properties listed above.

The algorithm proposed for source-seeking is the following: each robot moves according to a sum of two velocities:

$$\begin{aligned}\dot{X}_1 &= v_0\left(\vec{V}_{2\to 1}+\vec{V}_1\right)\\ \dot{X}_2 &= v_0\left(\vec{V}_{1\to 2}+\vec{V}_2\right)\end{aligned} \tag{1}$$

where v_0 is a normalization constant. By changing the velocity $\vec{V}_{j\to i}$, robot r_i seeks to maintain the desired distance from r_j by setting:

$$\vec{V}_{j\to i} = A_{ji}\cdot\hat{u}_{ij} \tag{2}$$

$$A_{ji} = \text{sign}\,(D-D_i)\in\{0,\pm 1\} \tag{3}$$

where the function sign (x) equals 1 if $x>0$; 0 if $x=0$; and -1 if $x<0$. Hence A_{ji} is the sign of the velocity. If $D>D_i$ then $A_{ji}=1$ so r_i is attracted toward r_j. If $D<D_i$ then $A_{ji}=-1$ so r_i is being repelled from r_j. If the robots would move only according to the velocities $\vec{V}_{2\to 1}$ and $\vec{V}_{1\to 2}$, they would forever travel along the line through their initial positions. To avoid that, the velocities $\vec{V}_1$ and $\vec{V}_2$ which cause the robots to orbit their center of mass are introduced. $\vec{V}_i$ is orthogonal to $\hat{u}_{ij}$ and is explicitly given by

$$\vec{V}_i = \hat{u}_{ij}\times\hat{u}_{up} \tag{4}$$

where $\hat{u}_{up}$ is the unit vector which points up (out of the plane).

3.1. Analysis of the source-seeking process

The algorithm is analyzed for the scenario in which the gradient of $z(\cdot)$ is constant in the vicinity of the robots, i.e. $\nabla z=\alpha\cdot\hat{u}$ where $\alpha>0$ is a constant and $\hat{u}$ is a unit vector. When the distance between the robots is not too large compared to the rate of change in $z(\cdot)$ the constant-gradient assumption is reasonable. Let θ be the angle between ∇z and $\hat{u}_{12}$, i.e. $\cos\theta=\hat{u}\cdot\hat{u}_{12}$. The notations $z_{CM}=z(CM)$, $D_{CM}=f(z_{CM})$ and $\dot{f}_{CM}=\left.\frac{df}{dz}\right|_{z=z_{CM}}$ are used in the analysis. Note that by f's definition, $0<\dot{f}_{CM}\cdot\alpha\le 1$.

Some consequences of the motion rules defined above on the time derivatives of four scalar values are presented in the following lemma:

Lemma 1. *During the execution of the source-seeking algorithm:*

1. $\dot{D}=-v_0(A_{12}+A_{21})$
2. $\dot{z}_{CM}=\frac{1}{2}v_0\alpha(A_{21}-A_{12})\cos\theta$
3. $\dot{D}_{CM}=\frac{1}{2}v_0\alpha\dot{f}_{CM}(A_{21}-A_{12})\cos\theta$
4. $\dot{\theta}=2v_0/D^2$

Proof. To prove 1,

$$\dot{D} = \frac{d}{dt}\sqrt{(X_2-X_1)(X_2-X_1)^T} \tag{5}$$

$$= \left(\dot{X}_2-\dot{X}_1\right)\cdot\hat{u}_{12} \tag{6}$$

$$= -v_0(A_{12}+A_{21}). \tag{7}$$

Next we have 2, since

$$\dot{z}_{CM} = \dot{CM}\cdot\nabla z=\frac{1}{2}\left(\dot{X}_1+\dot{X}_2\right)\cdot\alpha\hat{u} \tag{8}$$

$$= \frac{1}{2}v_0\alpha\left(\vec{V}_{1\to 2}+\vec{V}_1+\vec{V}_{2\to 1}+\vec{V}_2\right)\cdot\hat{u} \tag{9}$$

$$= \frac{1}{2}v_0\alpha(-A_{12}+A_{21})\cos\theta. \tag{10}$$

Using the chain rule, $\dot{D}_{CM}$ is given by

$$\dot{D}_{CM} = \dot{f}_{CM}\cdot\dot{z_{CM}}. \tag{11}$$

Substitution of $\dot{z_{CM}}$ concludes the proof of 3.

To prove the next result 4, consider the coordinate system defined by the two unit vectors $\hat{u}$ and $\hat{v}=\hat{u}_{up}\times\hat{u}$. The coordinates of the robots are given by (u_1,v_1) and (u_2,v_2). Using $\Delta v=v_2-v_1$, $\Delta u=u_2-u_1$ and $\tan\theta=\Delta v/\Delta u$ we get

$$\frac{1}{\cos^2\theta}\cdot\dot{\theta} = \frac{\Delta u\dot{\Delta v}-\Delta v\dot{\Delta u}}{\Delta u^2}. \tag{12}$$

The time derivatives are given by

$$\dot{\Delta v} = v_0 \left(\vec{V}_{1\to 2} - \vec{V}_{2\to 1} - 2\vec{V}_1\right) \cdot \hat{v} \tag{13}$$

$$\dot{\Delta u} = v_0 \left(\vec{V}_{1\to 2} - \vec{V}_{2\to 1} - 2\vec{V}_1\right) \cdot \hat{u}. \tag{14}$$

Substitution into Eq. (12) yields

$$\dot{\theta} = v_0 \cos^2\theta \frac{\left(\vec{V}_{1\to 2} - \vec{V}_{2\to 1} - 2\vec{V}_1\right)\left(\hat{v}\Delta u - \hat{u}\Delta v\right)}{\Delta x^2} \tag{15}$$

$$= v_0 \cos^2\theta \frac{\left((A_{21} + A_{12}) \cdot \hat{u}_{21} - 2\hat{u}_{12} \times \hat{u}_{up}\right)\left(-\hat{u}_{12} \times \hat{u}_{up}\right)}{\Delta u^2} \tag{16}$$

$$= 2\frac{v_0 \cos^2\theta}{\Delta u^2} = \frac{2v_0}{D^2} \tag{17}$$

where we have used $\hat{v}\Delta u - \hat{u}\Delta v = -\hat{u}_{12} \times \hat{u}_{up}$ and $\Delta u = D\cos\theta$. □

Let us next define the entropy (I) and potential (P) of the system, as follows

$$I = |D - D_{CM}| \tag{18}$$

$$P = 2z_{CM} - \alpha I. \tag{19}$$

Using Lemma 1, $\dot{P}$ is given by

$$\dot{P} = \begin{cases} v_0\alpha \left(\begin{array}{l} (A_{21} - A_{12})\cos\theta \left(1 + \frac{1}{2}\alpha \dot{f}_{CM}\right) \\ +A_{12} + A_{21} \end{array} \right) & D > D_{CM} \\ v_0\alpha \left(\begin{array}{l} (A_{21} - A_{12})\cos\theta \left(1 - \frac{1}{2}\alpha \dot{f}_{CM}\right) \\ -A_{12} - A_{21} \end{array} \right) & D \le D_{CM}. \end{cases} \tag{20}$$

Next we shall provide a lower bound on the rate of change of the potential:

Lemma 2. $\dot{P} \ge v_0\alpha \left(2 - \alpha \dot{f}_{CM}\right) |\cos\theta|$.

Proof. The following table covers all possible system states for the case where $D_2 > D_1$ ($\cos\theta > 0$). The elements of the last column are derived using Eq. (20).

	System state	A_{12}	A_{21}	$\dot{P}$
1	$D > D_2$	1	1	$2v_0\alpha$
2	$D = D_2$	0	1	$v_0\alpha \left(\cos\theta + 1 + \frac{1}{2}\alpha \dot{f}_{CM}\cos\theta\right)$
3	$D_{CM} < D < D_2$	−1	1	$v_0\alpha\cos\theta \left(2 + \alpha \dot{f}_{CM}\right)$
4	$D_1 < D \le D_{CM}$	−1	1	$v_0\alpha\cos\theta \left(2 - \alpha \dot{f}_{CM}\right)$
5	$D = D_1$	−1	0	$v_0\alpha \left(\cos\theta + 1 - \frac{1}{2}\alpha \dot{f}_{CM}\cos\theta\right)$
6	$D < D_1$	−1	−1	$2v_0\alpha$

For the 6 cases displayed above, using $0 < \alpha \dot{f}_{CM} \le 1$ and $\cos\theta = |\cos\theta|$ we get $\dot{P} \ge v_0\alpha \left(2 - \alpha \dot{f}_{CM}\right) |\cos\theta|$. Due to the system's symmetry, for $D_1 > D_2$, a similar table can be built yielding the same bound on $\dot{P}$.

To conclude the proof, consider $D_1 = D_2 = D_{CM}$ (i.e. $\cos\theta = 0$). If $D \ne D_{CM}$ then considering cases 1 or 6, $\dot{P} = 2\alpha v_0 \ge 0$. If $D = D_{CM}$ then $\dot{D} = \dot{D}_{CM} = 0$ hence $\dot{P} = 0$. □

Finally, we prove that z_{CM} continuously increases, hence the robots will drift toward higher $z(\cdot)$ values.

Theorem 3. *For any time t_0 and time interval Δt, we have:*

$$z_{CM}(t_0 + \Delta t) - z_{CM}(t_0) \ge \frac{v_0\alpha}{2} \int_{\tau=t_0}^{t_0+\Delta t} \left(2 - \alpha \dot{f}_{CM}\right) |\cos\theta| \, d\tau - \frac{1}{2}\alpha I(t_0). \tag{21}$$

Proof. Using the definition of P, let

$$z_{CM}(t_0 + \Delta t) - z_{CM}(t_0) = \frac{1}{2}\left[P(t_0 + \Delta t) + \alpha I(t_0 + \Delta t) - P(t_0) - \alpha I(t_0)\right] \tag{22}$$

$$= \frac{1}{2}\left[\int_{\tau=t_0}^{t_0+\Delta t} \dot{P} \cdot d\tau + \alpha I(t_0 + \Delta t) - \alpha I(t_0)\right]. \tag{23}$$

Since $I(t_0 + \Delta t)$ is positive we can write,

$$z_{CM}(t_0 + \Delta t) - z_{CM}(t_0) \geq \frac{1}{2}\left[\int_{\tau=t_0}^{t_0+\Delta t} \dot{P} \cdot d\tau - \alpha I(t_0)\right]. \tag{24}$$

Substitution of $\dot{P}$ from Lemma 2 concludes the proof. □

Theorem 3 implies that, as Δt increases, the difference $z_{CM}(t_0 + \Delta t) - z_{CM}(t_0)$ grows, hence the robots drift in the direction of increasing $z(\cdot)$. For example, let $t_0 = 0$ be the algorithm initialization time and assume that $z_{CM}(t_0) = 0$. By neglecting the constant term $I(t_0)$, Eq. (21) can be rewritten as

$$z_{CM}(t) \gtrapprox \frac{v_0\alpha}{2}\int_{\tau=0}^{t}\left(2 - \alpha\dot{f}_{CM}\right)|\cos\theta|\, d\tau. \tag{25}$$

The integrand in the right hand side of the equation above is positive, hence as t increases, $z_{CM}(t)$ grows, i.e. the value of the scalar function at the robots' center of mass increases. In other words, the robots drift with the gradient. Further discussion of implications of Theorem 3 can be found in Section 4.

Considering a linear f-function Theorem 3 can be restated as:

Corollary 4. *For $f(z) = \beta + \gamma z$, any time t_0 and time interval Δt,*

$$z_{CM}(t_0 + \Delta t) - z_{CM}(t_0) \geq \frac{v_0\alpha}{2}(2 - \alpha\gamma)\int_{\tau=t_0}^{t_0+\Delta t}|\cos\theta|\, d\tau - \frac{1}{2}\alpha I(t_0). \tag{26}$$

3.2. Robustness in case of noisy sensors

In this section, the algorithm is analyzed under the assumption of noisy sensors. It is assumed that the robots are able to measure their relative direction without error, i.e. the unit vectors $\hat{u}_{12}, \hat{u}_{21}$ are error-free. However, D and $z(\cdot)$ are measured with noise. As a result, the sign of the velocities $\vec{V}_{1\to2}$ and $\vec{V}_{2\to1}$ might occasionally be wrong resulting in attraction instead of repulsion or the other way around.

Let $\hat{z}_i$ and $\hat{D}$ be the values measured by robot r_i. We assume the following error model:

$$\hat{z}_i = z_i + N_z \tag{27}$$

$$\hat{D}_i = D + N_D \tag{28}$$

where N_z, N_D are random variables representing the measurement errors. It is assumed that N_z and N_D are symmetric and smooth, i.e. their probability measures obey the following for any x:

1. $Pr[N_z = x] = Pr[N_z = -x]$
2. $Pr[N_D = x] = Pr[N_D = -x]$
3. $Pr[x \leq N_z \leq x + \epsilon] = O(\epsilon)$
4. $Pr[x \leq N_D \leq x + \epsilon] = O(\epsilon)$

Smoothness (3 and 4) is assumed only for brevity, and a similar proof can be constructed without it. In this section, we shall limit the discussion to linear f-functions, i.e. $f(z) = \beta + \gamma \cdot z$ where $\beta \geq 0$ and $0 < \gamma \leq \frac{1}{\alpha}$ are constants. Let

$$\hat{I}_i = \hat{D}_i - f\left(\hat{z}_i\right) = D - D_i + N_I \tag{29}$$

where $N_I = N_D - \gamma N_z$ is a symmetric smooth random variable. The value of $\hat{I}_i$ will affect r_i's decision whether to move closer or away from r_j. Let $F_{N_I}(x)$ be the cumulative distribution function of N_I. Due to N_I's symmetry, for any $x \geq 0$, $F_{N_I}(x) \geq \frac{1}{2}$.

Let $\hat{A}_{ji}$ be the value used by robot r_i while executing the algorithm, i.e. when $\hat{I}_i > 0$ the robot employs $\hat{A}_{ji} = 1$ and when $\hat{I}_i < 0, \hat{A}_{ij} = -1$. Due to N_I's smoothness, the probability of $\hat{I}_i = 0$ is negligible. Let p_i be the probability that robot r_i is right in his choice whether to move closer or away from r_j, i.e. $p_i = Pr\left[\hat{A}_{ji} = A_{ji}\right]$. To calculate p_i, two cases are distinguished. In case $D - D_i > 0, A_{ji} = 1$ and

$$Pr\left[\hat{A}_{ji} = A_{ji} \,|\, A_{ji} = 1\right] = Pr\left[\hat{I}_i(D, z_i) > 0\right] \tag{30}$$

$$= Pr\left[D + N_i^D - f\left(z_i + N_i^z\right) > 0\right] \tag{31}$$

$$= Pr[I_i(D_i, z_i) > D_i - D] \tag{32}$$

$$= F_{N_I}(D - D_i). \tag{33}$$

In case $D - D_i < 0$ we get

$$Pr\left[\hat{A}_{ji} = A_{ji} \,|\, A_{ji} = -1\right] = Pr\left[\hat{I}_i\left(D, z_i\right) < 0\right] \tag{34}$$

$$= F_{N_I}\left(D_i - D\right). \tag{35}$$

Hence p_i is well defined, and given by

$$p_i = F_{N_I}\left(|D - D_i|\right). \tag{36}$$

Since $|D - D_i| \geq 0$ we have $p_i \geq \frac{1}{2}$.

Lemma 1 holds under our error model with A_{12} and A_{21} replaced by $\hat{A}_{12}$ and $\hat{A}_{21}$ respectively. Using $\dot{f}_{CM} = \gamma$, Eq. (20) can be written as

$$\dot{P} = \begin{cases} v_0\alpha\left(\begin{array}{l}\left(\hat{A}_{21} - \hat{A}_{12}\right)\cos\theta\left(1 + \frac{1}{2}\alpha\gamma\right)\\ +\hat{A}_{12} + \hat{A}_{21}\end{array}\right) & D > D_{CM} \\ v_0\alpha\left(\begin{array}{l}\left(\hat{A}_{21} - \hat{A}_{12}\right)\cos\theta\left(1 - \frac{1}{2}\alpha\gamma\right)\\ -\hat{A}_{12} - \hat{A}_{21}\end{array}\right) & D \leq D_{CM}. \end{cases} \tag{37}$$

By taking expectation w.r.t. the variables N_z and N_d (via N_I) we get

$$E\left[\dot{P}\right] = \begin{cases} v_0\alpha\left(\begin{array}{l}\left(A_{21}\left(2p_1 - 1\right) - A_{12}\left(2p_2 - 1\right)\right)\\ \cdot\cos\theta\left(1 + \frac{1}{2}\alpha\gamma\right)\\ +A_{12}\left(2p_2 - 1\right) + A_{21}\left(2p_1 - 1\right)\end{array}\right) & D > D_{CM} \\ v_0\alpha\left(\begin{array}{l}\left(A_{21}\left(2p_1 - 1\right) - A_{12}\left(2p_2 - 1\right)\right)\\ \cdot\cos\theta\left(1 - \frac{1}{2}\alpha\gamma\right)\\ -A_{12}\left(2p_2 - 1\right) - A_{21}\left(2p_1 - 1\right)\end{array}\right) & D \leq D_{CM} \end{cases} \tag{38}$$

where we have used $E\left[\hat{A}_{ji}\right] = A_{ji}\left(2p_i - 1\right)$.

Lemma 5. $E\left[\dot{P}\right] \geq v_0\alpha\left(p_1 + p_2 - 1\right)\left(2 - \alpha\gamma\right)|\cos\theta|$.

Proof. Similarly to the proof of Lemma 2 let $D_2 > D_1$. The elements of the last column of the table below are derived using Eq. (38).

	System state	A_{12}	A_{21}	$E\left[\dot{P}\right]$
1	$D > D_2$	1	1	$v_0\alpha\left(\begin{array}{l}\left(p_1 - p_2\right)\cos\theta\left(2 + \alpha\gamma\right)\\ +2\left(p_2 + p_1 - 1\right)\end{array}\right)$
2	$D_{CM} < D < D_2$	-1	1	$v_0\alpha\left(\begin{array}{l}\left(p_1 + p_2 - 1\right)\cos\theta\left(2 + \alpha\gamma\right)\\ +2\left(p_1 - p_2\right)\end{array}\right)$
3	$D_1 < D \leq D_{CM}$	-1	1	$v_0\alpha\left(\begin{array}{l}\left(p_1 + p_2 - 1\right)\cos\theta\left(2 - \alpha\gamma\right)\\ +2\left(p_2 - p_1\right)\end{array}\right)$
4	$D < D_1$	-1	-1	$v_0\alpha\left(\begin{array}{l}\left(p_2 - p_1\right)\cos\theta\left(2 - \alpha\gamma\right)\\ +2\left(p_1 + p_2 - 1\right)\end{array}\right)$

For a linear f-function, $D_{CM} = \frac{1}{2}\left(D_1 + D_2\right)$. For states 1 and 2, $D > D_{CM}$. Hence $|D - D_2| < |D - D_1|$ and $p_2 = F_{N_I}\left(|D - D_2|\right) \leq F_{N_I}\left(|D - D_1|\right) = p_1$. Using $p_2 \leq p_1$, $\alpha\gamma \leq 1$ and $\cos\theta = |\cos\theta|$, $E\left[\dot{P}\right]$ of states 1 and 2 can be bounded by $v_0\alpha\left(p_1 + p_2 - 1\right)\left(2 - \alpha\gamma\right)|\cos\theta|$. For states 3 and 4, $|D - D_1| \leq |D - D_2|$ so $p_1 \leq p_2$ and $E\left[\dot{P}\right]$ can be bounded similarly.

For $D_1 > D_2$, due to the system's symmetry, a similar table can be constructed yielding the same bound on $\dot{P}$. To conclude the proof consider $D_1 = D_2 = D_{CM}$ (i.e. $\cos\theta = 0$). If $D \neq D_{CM}$ then according to states 1 and 4, $\dot{P} \geq 2v_0\left(p_2 + p_1 - 1\right) \geq 0$. If $D = D_{CM}$ then $\dot{D} = \dot{D}_{CM} = 0$, hence $\dot{P} = 0$. □

The following theorem is a result similar to Theorem 3, under noisy observations:

Theorem 6. *For any linear f-function, time t_0 and time interval Δt,*

$$E\left[z_{CM}\left(t_0 + \Delta t\right)\right] - z_{CM}\left(t_0\right) \geq \frac{v_0\alpha}{2}\left(2 - \alpha\gamma\right)\int_{t=t_0}^{t_0+\Delta t}\left(p_1 + p_2 - 1\right)|\cos\theta|\,dt - \frac{1}{2}I\left(t_0\right). \tag{39}$$

Proof. Using the definition of P, and $I(t_0 + \Delta t) \geq 0$ we write,

$$z_{CM}(t_0 + \Delta t) - z_{CM}(t_0) \geq \frac{1}{2}\left[\int_{\tau=t_0}^{t_0+\Delta t} E\left[\dot{P}\right] \cdot d\tau - \alpha I(t_0)\right]. \tag{40}$$

Substitution of the lower bound on $E\left[\dot{P}\right]$ from Lemma 5 concludes the proof. □

The bound above equals the bound given in Theorem 3 multiplied by the term $(p_1 + p_2 - 1)$. In case the sensing errors are negligible we have $p_1 = p_2 = 1$ and the two bounds agree. In case the robots frequently err in choosing $\hat{A}_{12}$ and $\hat{A}_{21}$, p_1 and p_2 are smaller so the robots follow the gradient slower. Nevertheless, in any case, $p_1 + p_2 - 1 \geq 0$, hence the expected direction of the drift is toward high values. The probability p_i is a complex function of $D, f(z_i)$ and the distribution of N_I, see Eq. (36). Nevertheless, the following lemma provides a crude lower bound for the term $p_1 + p_2 - 1$.

Lemma 7. $p_1 + p_2 - 1 \geq \left(F_{N_I}\left(\frac{\alpha\beta\gamma}{2+\alpha\gamma}|\cos\theta|\right) - \frac{1}{2}\right)$.

Proof. Let $\Delta D_{\max} = \max\{|D - D_1|, |D - D_2|\}$. Recall that $f(z) = \beta + \gamma z$. For $D \leq \frac{2\beta}{2+\alpha\gamma}$ we have $\Delta D_{\max} \geq \beta - D \geq \frac{\alpha\beta\gamma}{2+\alpha\gamma}$. For a linear f-function,

$$|D_2 - D_1| = \gamma|z_2 - z_1| = \alpha\gamma D|\cos\theta|. \tag{41}$$

Using the triangle inequality $\Delta_{\max} \geq \frac{1}{2}\alpha\gamma D|\cos\theta|$. For $D \geq \frac{2\beta}{2+\alpha\gamma}$ we get $\Delta_{\max} \geq \frac{\alpha\beta\gamma}{2+\alpha\gamma}|\cos\theta|$. Hence for any D, $\Delta_{\max} \geq \frac{\beta\alpha\gamma}{2+\gamma}|\cos\theta|$. Using Eq. (36),

$$p_1 + p_2 - 1 = F_{N_I}(|D - D_1|) + F_{N_I}(|D - D_2|) - 1 \tag{42}$$

$$\geq \left[F_{N_I}(\Delta D_{\max}) - \frac{1}{2}\right] + \left[F_{N_I}(0) - \frac{1}{2}\right] \tag{43}$$

$$\geq F_{N_I}\left(\frac{\alpha\beta\gamma}{2+\alpha\gamma}|\cos\theta|\right) - \frac{1}{2} \tag{44}$$

where we have used $F_{N_I}(0) \geq \frac{1}{2}$. □

Substitution of the result of Lemma 7 into the bound given in Theorem 6 yields the corollary to be stated below. Note that the bound given in Lemma 7 is not tight. As a result, the bound given in Corollary 8 is not tight. Hence the corollary is a proof of the correctness of the algorithm and does not yield a precise prediction of the speed of drift.

Corollary 8. *For any linear f-function, time t_0 and time interval Δt,*

$$E[z_{CM}(t_0 + \Delta t)] - z_{CM}(t_0) \geq \frac{1}{2}v_0\alpha(2 - \alpha\gamma)\int_{\tau=t_0}^{t_0+\Delta t}\left(F_{N_I}\left(\frac{\beta\alpha\gamma}{2+\gamma}|\cos\theta|\right) - \frac{1}{2}\right)|\cos\theta|\,d\tau - \frac{1}{2}I(t_0). \tag{45}$$

Let $\Delta = D - \max\{D_1, D_2\}$. The following lemma shows that when the probabilities p_1, p_2 are high enough, the system tends to be in a state where $\Delta \leq 0$, i.e. $D \leq \max\{D_1, D_2\}$. The implications of this result will be discussed in the next section.

Lemma 9. *If $\Delta > 0$ then $E\left[\dot{\Delta}\right] \leq -2v_0\left(p_1 + p_2 - 1 - \frac{1}{\sqrt{2}}\alpha\gamma\right)$.*

Proof. Consider $\Delta > 0$. Since $D > \max\{D_1, D_2\}$, $A_{12} = A_{21} = 1$. The maximum speed of each of the robots is $\sqrt{2}v_0$, hence $\left|\dot{D}_i\right| \leq \sqrt{2}v_0\alpha\gamma$. Using $\dot{D}$ from Lemma 1 we write

$$E\left[\dot{\Delta}\right] \leq E\left[-v_0\left(\hat{A}_{12} + \hat{A}_{21}\right) + \sqrt{2}v_0\alpha\gamma\right] \tag{46}$$

$$= -2v_0\left(p_1 + p_2 - 1 - \frac{1}{\sqrt{2}}\alpha\gamma\right). \quad \square \tag{47}$$

4. Discussion and simulations

As we have seen in previous sections, a linear f-function enables a rather complete analysis of the source-seeking algorithm. Hence only linear functions will be considered further in this section.

Corollary 4 bounds the speed of drift toward high values for the errorless case. Before testing the tightness of the bound, a simple approximation is provided. Using the initial conditions $t_0 = 0$ and $z_{CM}(0) = 0$, the bound of Corollary 4 can be rewritten as follows

$$z_{CM}(t) \geq \frac{v_0\alpha}{2}(2 - \alpha\gamma)\int_{\tau=0}^{t}|\cos\theta|\,d\tau - \frac{1}{2}\alpha I(0). \tag{48}$$

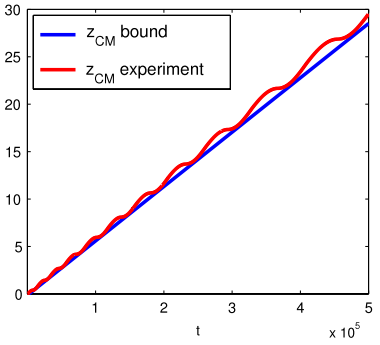

(a) The time course of z_{CM}.

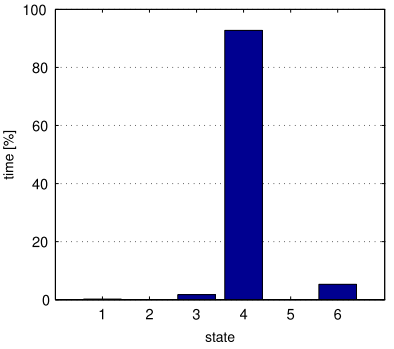

(b) The amount of time spent in each of the system states (as defined in Lemma 2).

Fig. 2. Simulation results for $f(z) = 1 + 0.2z$, $\alpha = 1$ and accurate sensors.

By Lemma 1, $\dot{\theta} = v_0/D^2$ where D is time varying. Nevertheless, in order to further simplify the bound, by assuming that D varies slowly compared to v_0, $\dot{\theta}$ can be approximated by a constant, i.e. $\dot{\theta} \simeq \omega_0$. For $t \gg \omega_0$,

$$z_{CM}(t) \gtrapprox \frac{v_0\alpha}{2}(2-\alpha\gamma)\int_{\tau=0}^{t}\left|\cos\left(\omega_0 t'\right)\right| d\tau - \frac{1}{2}\alpha I(0) \tag{49}$$

$$\simeq \frac{v_0\alpha}{2}(2-\alpha\gamma)\cdot\frac{t}{\pi}\cdot\int_{\theta=-\frac{1}{2}\pi}^{\frac{1}{2}\pi}|\cos\theta|\, d\theta - \frac{1}{2}\alpha I(0) \tag{50}$$

$$= (2-\alpha\gamma)\frac{v_0\alpha}{\pi}t - \frac{1}{2}\alpha I(0). \tag{51}$$

So the average growth rate of z_{CM} is bounded from below by $(2-\alpha\gamma)\frac{v_0\alpha}{\pi}$.

In order to examine the simplified bound above, computer simulations were performed in an environment in which $z(X) = \alpha \cdot x$ where x is the x-coordinate of point X and α is a constant. Thus for any point X, $\nabla z(X) = \alpha \cdot \hat{x}$ where $\hat{x}$ is the x-axis unit vector. Extensive tests were performed with varying α, β and γ. In all cases the bound was found to be tight, i.e. Corollary 4 predicts the speed of gradient climbing well. An example of an experimental result is displayed in Fig. 2. The time course of z_{CM} is presented in Fig. 2a and a histogram specifying the amount of time spent in each of the system states (as defined in Lemma 2) is presented in Fig. 2b. The accuracy of the bound results from the fact that about 94% of the time the system was in state 4, i.e. the state for which $\dot{P}$ is bounded tightly, see Lemma 2. To summarize, the lower bound on the speed of drift toward high values for the errorless case provided in Corollary 4 was found to be tight in our experiments, i.e. it has predicted the gradient climbing speed well.

In order to examine the tightness of the bound for the noisy sensors case, a similar approximation is used for the bound given in Corollary 8. Considering the initial conditions $t_0 = 0$ and $z_{CM}(0) = 0$, the bound given in Corollary 8 can be written as follows:

$$E[z_{CM}(t)] \geq \frac{v_0\alpha}{2}(2-\alpha\gamma)\int_{\tau=0}^{t}\left(F_{N_I}\left(\frac{\beta\alpha\gamma}{2+\gamma}|\cos\theta|\right)-\frac{1}{2}\right)|\cos\theta|\, d\tau - \frac{1}{2}I(t_0). \tag{52}$$

The approximation $\dot{\theta} = \omega_0$ yields

$$E[z_{CM}(t)] \gtrsim \frac{v_0\alpha(2-\alpha\gamma)}{2\pi}t\int_{\theta=-\frac{1}{2}\pi}^{\frac{1}{2}\pi}\left(F_{N_I}\left(\frac{\beta\alpha\gamma}{2+\gamma}|\cos\theta|\right)-\frac{1}{2}\right)|\cos\theta|\, d\theta - \frac{1}{2}I(t_0). \tag{53}$$

For a given distribution of N_I, the integral above can be calculated numerically. Simulations were again performed considering a normally distributed N_I with a variance of σ_I^2. The results are presented in Fig. 3. In contradiction with the tightness of the lower bound for the noise-free case, in the noisy scenario the algorithm performs much better than the given bound. That is because the term $p_1 + p_2 - 1$ is bounded quite pessimistically in Lemma 7. Due to the complexity of these probabilities, we could not find a tighter bound. However, a better bound on $p_1 + p_2 - 1$, in case such a bound exists, will improve the result of Corollary 8. Another interesting result is that the speed of drifting with the gradient was found to be inversely proportional to the amount of noise (σ_I^2). That is due to the fact that when σ_I^2 is higher, the robots tend to move in the wrong direction more frequently.

Real life robots also have a limited sensing range. Hence, to guarantee proper system behavior it is required to limit the distance between the robots. Recall that $\Delta = D - \max\{D_1, D_2\}$. By Lemma 9, if $\Delta > 0$ (assuming $p_1 + p_2 - 1 - \frac{\alpha}{\sqrt{2}}\gamma > 0$) then $E\left[\dot{\Delta}\right] < 0$. Hence, we would expect Δ to be negative, i.e. $D \leq \max\{D_1, D_2\}$. The simulations agree: according to the histograms in Figs. 2 and 3 the system was almost never in state 1, i.e. the only state in which $D > \max\{D_1, D_2\}$. Hence the

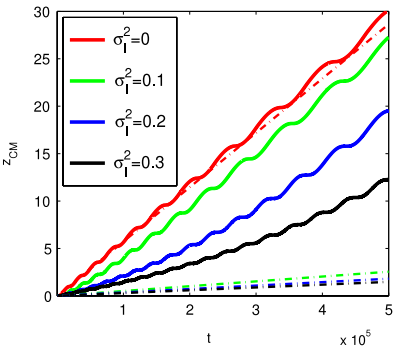

(a) The solid lines are the experimental results and the dashed lines are the bounds as given in Eq. (53).

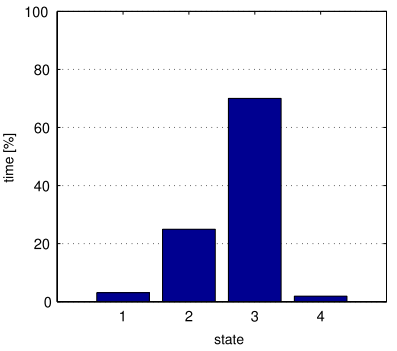

(b) The amount of time spent in each of the system states (as defined in Lemma 5) for $\sigma_l^2 = 0.3$.

Fig. 3. Simulation results for $f(z) = 1 + 0.2z$, $\alpha = 1$ and N_l distributed normally with a variance of σ_l^2.

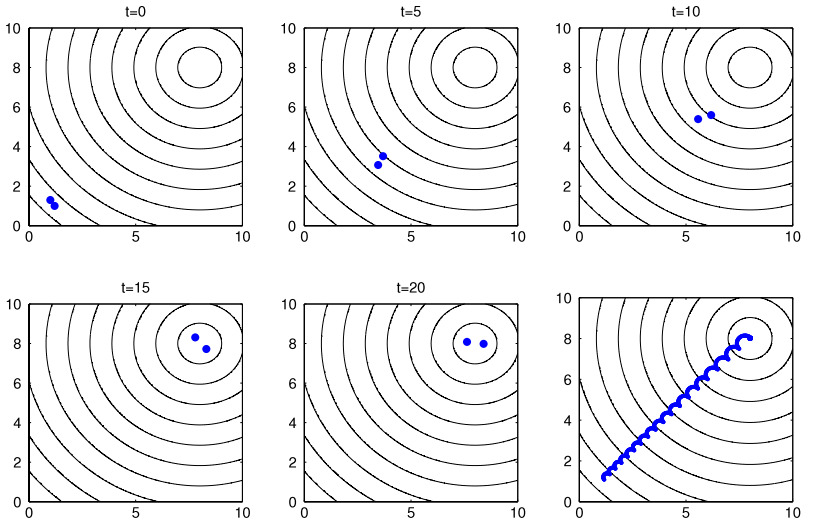

Fig. 4. Simulation in a simple environment comprising a single maximum. The contours represent the scalar function and the circular markers are the robots. The path of the robots' center of mass is presented in the bottom right subfigure. In the experiment, the robots found the maxima and circled it.

distance between the robots can be bounded by $\max\{D_1, D_2\}$. Let $f_{\max}$ be the maximum value f reaches in the environment, i.e. $f_{\max} = \beta + \gamma \max\{z\}$. Clearly, $\max\{D_1, D_2\} \leq f_{\max}$. So a proper inter-robot distance can be guaranteed by designing an f-function for which $f_{\max}$ will be smaller than the robot's visibility range.

Recall that the algorithm was analyzed under the assumption of a constant gradient. The constant gradient assumption was justified by the small dimensions of the robots and the small distance between them: we would expect that the weak gradient of the scalar function will be roughly constant in the small surroundings of the robots. Extensive simulations were performed in order to validate this assumption. Note that the proposed algorithm is a gradient climbing algorithm hence cannot escape local maxima (as any other gradient climbing algorithm). Thus only environments without local maxima were examined. In all experiments the robots successfully found the maxima of the signal and circled it. Observe Fig. 4 for the results of a simulation in a simple environment containing a single maximum. The path of the robots' center of mass is presented in the bottom right subfigure (of Fig. 4). In all experiments, the path was found to be serrated rather than straight, thus, in agreement with the $|\cos\theta|$ component of Theorems 3 and 6. The results of an experiment in a more complex environment are presented in Fig. 5.

5. Conclusion

In this paper a two-robot *reactive* gradient-following algorithm for memoryless robots performing point measurements was presented. Using indirect motion based communication, the robots implicitly "compare their point measurements" and drift with the gradient. We have proved that in case the gradient is constant in the vicinity of the robots, the algorithm is correct assuming accurate or noisy sensors.

The main open issue is how to extend the algorithm to larger groups of robotic agents. We have successfully designed a source-seeking procedure for a three-robot system in which the robots attempt to form a equilateral triangle and follow

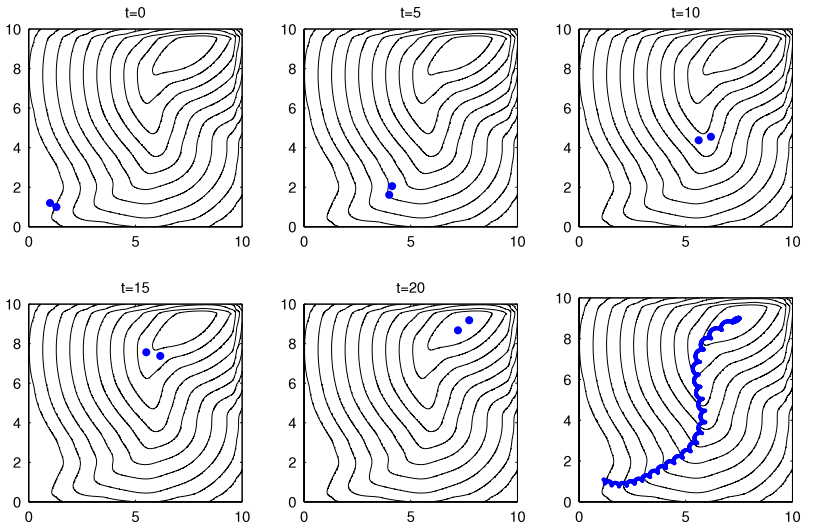

Fig. 5. Simulation in a complex environment comprising a single maximum. The contours represent the scalar function and the circular markers are the robots. The path of the robots' center of mass is presented in the bottom right subfigure. In the experiment, the robots found the maxima and circled it.

the gradient. Considering much larger groups, we believe that full mutual visibility is not a reasonable assumption. Therefore, we are currently working on a distributed source-seeking process assuming every robot is able to sense only nearby robots.

Acknowledgments

We thank the anonymous reviewers for their valuable comments that helped us improve the paper.

References

[1] B.J. Moore, C. Canudas de Wit, Source seeking via collaborative measurements by a circular formation of agents, in: American Control Conf. (ACC), Jul. 2010, pp. 6417–6422.
[2] G. Kowadlo, R.A. Russell, Robot odor localization: a taxonomy and survey, The International Journal of Robotics Research 27 (8) (2008) 869–894.
[3] E. Burian, D. Yoerger, A. Bradley, H. Singh, Gradient search with autonomous underwater vehicles using scalar measurements, in: Proc. of the 1996 Symp. on Autonomous Underwater VehicleTechnology, AUV'96, 1996, pp. 86–98.
[4] E. Biyik, M. Arcak, Gradient climbing in formation via extremum seeking and passivity-based coordination rules, in: 46th IEEE Conf. on Decision and Control, 2007, pp. 3133–3138.
[5] Wencen Wu, Fumin Zhang, Curvature based cooperative exploration of three dimensional scalar fields, in: American Control Conference, ACC, 2010, 30 2010–july 2 2010, pp. 2909 –2914.
[6] O. Holland, C. Melhuish, Some adaptive movements of animats with single symmetrical sensors, in: Proc. of the Fourth Int. Conf. on Simulation of Adaptive behavior, pp. 55–64.
[7] R.A. Russell, Robotic location of underground chemical sources, Robotica 22 (01) (2004) 109–115.
[8] D.A. Hoskins, Least action approach to collective behavior, in: Proc SPIE. Microrobotics and Micromechanical Systems, vol. 2593, 1995, pp. 108–120.
[9] R.A. Russell, Locating underground chemical sources by tracking chemical gradients in 3 dimensions, in: IEEE/RSJ Int. Conf. on Intel. Robots and Systems, IROS 2004, vol. 1, 2004, pp. 325–330.
[10] C.G. Mayhew, R.G. Sanfelice, A.R. Teel, Robust source-seeking hybrid controllers for autonomous vehicles, in: American Control Conf., ACC'07, 2007, pp. 1185–1190.
[11] C.G. Mayhew, R.G. Sanfelice, A.R. Teel, Robust hybrid source-seeking algorithms based on directional derivatives and their approximations, in: 47th IEEE Conf. on Decision and Control, CDC 2008, 2008, pp. 1735–1740.
[12] A.S. Matveev, H. Teimoori, A.V. Savkin, Navigation of a non-holonomic vehicle for gradient climbing and source seeking without gradient estimation, in: American Control Conf., ACC, July 2010, pp. 219–223.
[13] A.S. Matveev, H. Teimoori, A.V. Savkin, Navigation of a unicycle-like mobile robot for environmental extremum seeking, Automatica 47 (1) (2011) 85–91.
[14] J. Cochran, M. Krstic, Nonholonomic source seeking with tuning of angular velocity, IEEE Transactions on Automatic Control 54 (4) (2009) 717–731.
[15] S. Liu, M. Krstic, Stochastic source seeking for nonholonomic unicycle, Automatica 46 (9) (2010) 1443–1453.
[16] J. Cochran, A. Siranosian, N. Ghods, M. Krstic, 3-d source seeking for underactuated vehicles without position measurement, IEEE Transactions on Robotics 25 (1) (2009) 117–129.
[17] C. Zhang, D. Arnold, N. Ghods, A. Siranosian, M. Krstic, Source seeking with non-holonomic unicycle without position measurement and with tuning of forward velocity, Systems & Control Letters 56 (3) (2007) 245–252.
[18] O. Khatib, Real-time obstacle avoidance for manipulators and mobile robots, The International Journal of Robotics Research 5 (1) (1986) 90–98.
[19] V. Gazi, K.M. Passino, Stability analysis of social foraging swarms, IEEE Transactions on Systems, Man, and Cybernetics, Part B: Cybernetics 34 (1) (2004) 539–557.
[20] P. Ogren, M. Egerstedt, X. Hu, A control lyapunov function approach to multi-agent coordination, in: Proc. of the 40th IEEE Conf. on Decision and Control, vol. 2, 2001, pp. 1150–1155.
[21] P. Ogren, E. Fiorelli, N.E. Leonard, Cooperative control of mobile sensor networks: adaptive gradient climbing in a distributed environment, IEEE Transactions on Automatic Control 49 (8) (2004) 1292–1302.
[22] R. Bachmayer, N.E. Leonard, Vehicle networks for gradient descent in a sampled environment, in: Proc. of the 41st IEEE Conf. on Decision and Control, vol. 1, 2002, pp. 112–117.
[23] N. Ghods, M. Krstic, Multiagent deployment over a source, IEEE Transactions on Control Systems Technology 20 (1) (2012) 277–285.
[24] A. Mesquita, J. Hespanha, K. Astrom, Optimotaxis: a stochastic multi-agent optimization procedure with point measurements, in: Hybrid Systems: Computation and Control, vol. 4981, 2008, pp. 358–371.